

NEW HORIZONS IN MODELING AND SIMULATION OF ELECTROSPUN NANOFIBERS: A DETAILED REVIEW

S. RAFIEI, S. MAGHSOODLOO, M. SABERI, S. LOTFI, V. MOTAGHITALAB,
B. NOROOZI and A. K. HAGHI

University of Guilan, Rasht, Iran

✉ *Corresponding author: A. K. Haghi, akhaghi@yahoo.com*

Received June 8, 2013

Electrospinning is applied to create continuous fibers with nanometer diameters through jetting polymer solutions in high electric fields. A drawback of this method, however, is the unstable behavior of the liquid jet, which causes the fibers to be collected randomly. So a critical concern in this process is to achieve desirable control. Studying the dynamics of the electrospinning jet will be easier and faster, if it can be modeled and simulated, rather than doing experiments. This paper focuses on modeling and then simulating the electrospinning process as viewed by different approaches. In order to study the applicability of the electrospinning modeling equations, which have been discussed in detail in earlier parts of this review, an existing mathematical model, in which the jet is considered as a mechanical system, has been interconnected with viscoelastic elements and used to build a numeric method. The simulation features the possibility of predicting essential parameters of the electrospinning process and the results are in good agreement with those of other numeric studies of electrospinning, which modeled this process based on axial direction.

Keywords: electrospinning, electrospinning modeling, electrospinning simulation

INTRODUCTION

Electrospinning is a procedure, in which an electrical charge is applied to draw very fine (typically in the micro- or nanoscale) fibers from polymer solution or melt. Electrospinning shares characteristics of both electro spraying and conventional solution dry spinning of fibers. The process does not require the use of coagulation chemistry or high temperature operations for manufacturing solid threads from solution. This makes it more efficient to produce polymeric fibers with large and complex molecules. Recently, various polymers have been successfully electrospun into ultrafine fibers mostly in solvent solution and some in melt form.¹⁻² Optimization of the alignment and morphology of the fibers is produced by fitting the composition of the solution and the configuration of the electrospinning apparatus, such as voltage, flow rate, and etc. As a result, the efficiency of this method can be improved.³ Mathematical and theoretical modeling and simulating procedure will assist in offering an in-depth insight into the physical understanding of complex phenomena during electrospinning and

might be very applicable to manage contributing factors toward increasing the production rate.⁴⁻⁵

Despite the simplicity of the electrospinning technology, industrial applications of this method are still relatively rare, mainly due to the notable problems of very low fiber production rate and difficulties in controlling the process.⁶

Modeling and simulation (M&S) yield appropriate information about how something will act without actual testing in real. Modeling is a representation of a real object or system of objects for purposes of visualizing its appearance or analyzing its behavior. Simulation is transition from a mathematical or computational model to the description of the system behavior based on sets of input parameters.⁷⁻⁸ It is often the only means for accurately predicting the performance of the modeled system.⁹ Using simulation is generally cheaper and safer than conducting experiments with a prototype of the final product. In addition, in experimental situations when the possibility of error is high, simulation can be even more realistic than experiments, as they allow the free configuration of environmental and ope-

rational parameters and is able to be run faster than in real time. In a situation with different alternatives analysis, simulation can improve the efficiency, particularly when the necessary data for initializing can easily be obtained from operational data. Finally, applying simulation adds decision support systems to the toolbox of traditional decision support systems.¹⁰

Simulation permits to arrange a coherent synthetic environment, which allows the integration of systems in the early analysis phase for a virtual test environment in the final system. Managing correctly, the environment can be migrated from the development and test domain to the training and education one in a real system under practical constraints.¹¹

A collection of experimental data and their confrontation with simple physical models appears as an effective approach towards the development of practical tools for controlling and optimizing the electrospinning process. On the other hand, it is necessary to develop theoretical and numerical models of electrospinning, because each material demands a different optimization procedure.¹² Utilizing a model to express the effect of electrospinning parameters will assist researchers in making an easy and systematic way of presenting the influence of variables and by means of that, the process can be controlled. Additionally, predicting the results under a new combination of parameters becomes possible. Therefore, without conducting any experiments, one can easily estimate features of the product under unknown conditions.¹³

ELECTROSPINNING

Spinning is the processes applied for drawing fiber from a polymer into filaments by passing through a spinneret, which is classified into solution (wet or dry) and melt spinning. Conventional fiber-forming techniques possess various limitations including lack of sufficient control on fiber diameters, due to their dependency on the properties of the devices used, such as spinneret diameter. As mentioned earlier, the major technique to make fibers thinner than 100 μm is electrospinning, which is capable of giving very long continuous fibers by electrostatically drawing a polymer jet through a virtual spatio-temporal orifice.¹⁴ An overview of the invention history of this technique is reported herein and then the principle of the electrospinning methodology is discussed.

History of the science and technology of electrospinning

William Gilbert discovered the first record of the electrostatic attraction of a liquid in 1600.¹⁵ The first electrospinning patent was submitted by John Francis Cooley in 1900.¹⁶ Succeeding that, in 1914, John Zeleny studied the behavior of fluid droplets at the end of metal capillaries, which caused the beginning of the mathematically modeling of fluids behavior under electrostatic forces.¹⁷ Between 1931 and 1944, Anton Formhals obtained at least 22 patents on electrospinning.¹⁶ Thereinafter, in 1938, N.D. Rozenblum and I. V. Petryanov-Sokolov generated electrospun fibers, which they developed into filter materials.¹⁸ Between 1964 and 1969, Sir Geoffrey Ingram Taylor marked the beginnings of a theoretical foundation of electrospinning by mathematically modeling the shape of the (Taylor) cone formed by the fluid droplet under the effect of an electric field.¹⁹⁻²⁰ In the early 1990s, several research groups (such as Reneker's) demonstrated electrospun nanofibers. Since 1995, the number of publications about electrospinning has been increasing exponentially every year.¹⁶

Basic principles of electrospinning

As indicated above, electrospinning is a simple and easily controlled technique that provides the possibility of forming fibers with dimensions down to the nanometer range. Electrospinning fiber precursors are classified into spinnable polymers and other materials, such as metals, ceramics, and glasses. During a typical electrospinning experiment in a laboratory, a polymer solution or melt is pumped through a thin nozzle with an inner diameter of the order of 100 μm . In most of laboratory systems, the nozzle simultaneously serves as an electrode, to which a high electric field of 100-500 $\text{kV}\cdot\text{m}^{-1}$ is applied, and the distance to the counter electrode is of 10-25 cm .²¹ The currents that flow during electrospinning range from a few hundred nanoamperes to microamperes. A high voltage is applied to the solution, so that at a critical voltage, typically more than 5 kV , the repulsive force within the charged solution is larger than the surface tension, as a result, a fluid jet would erupt from the tip of the spinneret. Although the jet is stable near to the tip of the spinneret, it would enter a bending instability stage with further stretching of the solution jet under the electrosta-

tic forces as the solvent evaporates.²²⁻²³ The substrate on which the electrospun fibers are collected is typically brought into contact with the counter electrode that are rotating or flat types.²² The vertical alignment of the electrodes “from top

to bottom” is not very usual with respect to the process and in principal, electrospinning is usually carried out “from bottom to top” or horizontally.

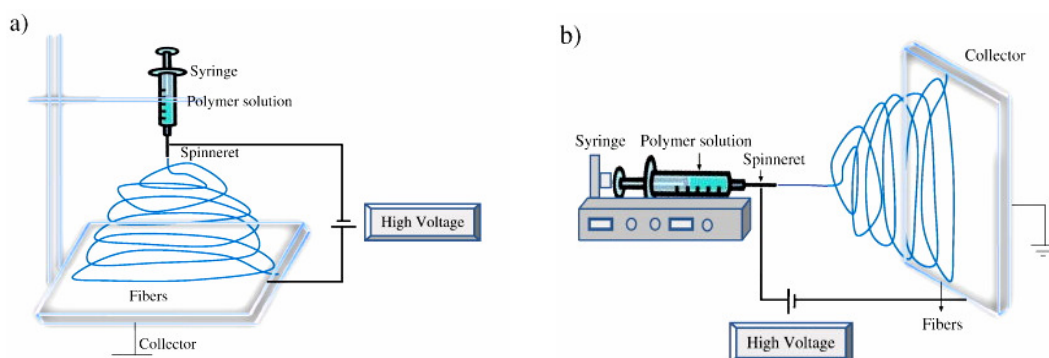


Figure 1: Electrospinning set-ups: a) vertical alignment of the electrodes (top to bottom design), b) horizontal alignment (bottom to top design)

Table 1
Classification of affecting parameters and nozzle configuration types on electrospinning

| Affecting parameters | | |
|--|---------------------------------|--------------------|
| Process parameters | System parameters | Ambient parameters |
| ✓ electric potential | ✓ molecular weight | ✓ temperature |
| ✓ flow rate | ✓ molecular weight distribution | ✓ humidity |
| ✓ concentration | ✓ architecture of the polymer | ✓ air velocity |
| ✓ spinning distance | | |
| Type of electrospinning nozzle configuration | | |
| | ✓ single | |
| | ✓ side by side | |
| | ✓ co-axial | |

Both electrospinning set-ups are presented in Fig. 1.²⁴ The formation of nanofibers is determined by many operating parameters, which are included in Table 1.

MODELING AND SIMULATION CONCEPTS

Numerous processing operations of complex fluids involve free surface deformations, such as spraying and atomization of fertilizers and pesticides, fiber-spinning operations, paint application, roll-coating of adhesives and food processing operations. These numerical approaches have been investigated widely by means of modeling and subsequent simulation. Systematical understanding of flows behaviour in processes such as electrospinning can be extremely difficult because of the variation of different forces that may be involved, including capillarity, viscosity, inertia, gravity, as well as

the additional stresses resulting from the extensional deformation of the microstructure within the fluid.²⁵

Theoretical and numerical comprehension of these phenomena can assist in overcoming the existing restrictions throughout the process. For example, as regards this approach, in spite of individual applications of the electrospinning process, its mass production is still a challenge.⁶ For achieving higher mass production and nanofibers orientation for special application, like tissue engineering and microelectronics, it is necessary to comprehend and control the dynamic and mechanic behavior of the electrospinning jet.²⁶⁻²⁷ Modeling and simulations will offer a better understanding of the electrospinning jet mechanics and dynamics. For example, the effect of secondary external field can be surveyed using simulation studies. As well, poor deposition

control may be in part caused by the lack of understanding of the mechanisms of dynamic interactions of the fast moving jets with the electric field and collectors.²⁷ Electrospinning modeling and simulation are discussed in detail in the following sections.

Electrospinning modeling

The electrospinning process is a fluid dynamics related problem and its thorough study requires a numerical and mathematical vision. Controlling the property, geometry, and mass production of the nanofibers, is essential to comprehend quantitatively how the electrospinning process transforms the fluid solution through a millimeter diameter capillary tube into solid fibers, which are four to five orders smaller in diameter.²⁸ Although information on the effect of various processing parameters and constituent material properties can be obtained experimentally, theoretical models offer in-depth scientific understanding, which can be useful to clarify the affecting factors that cannot be exactly measured experimentally. Results from modeling also explain how processing parameters and fluid behavior lead to nanofibers with appropriate properties. The term "properties" refers to basic properties (such as fiber diameter, surface roughness, fiber connectivity, etc.), physical properties (such as stiffness, toughness, thermal conductivity, electrical resistivity, thermal expansion coefficient, density, etc.) and specialized properties (such as biocompatibility, degradation curve, etc. for biomedical applications).^{23, 29}

For instance, various developed models can be employed for the analysis of jet deposition and alignment mechanisms on different collecting devices in arbitrary electric fields.²⁷

Several methods formulated by researchers are prompted by various applications of nanofibers. It would be sufficient to briefly describe some of these methods to observe the similarities and disadvantages of these approaches. An abbreviated literature review of these models will be discussed below.

Electrospinning simulation

Electrospun polymer nanofibers demonstrate outstanding mechanical and thermodynamic properties, as compared to macroscopic-scale structures. These features are attributed to nanofiber microstructure.³⁰⁻³¹ Theoretical

modeling predicts the nanostructure formations during electrospinning.

This prediction could be verified by various experimental conditions and analysis methods, which are called simulation. Numerical simulations can be compared with experimental observations as the last evidence.^{27, 32}

Parametric analysis and accounting complex geometries in the simulation of electrospinning are extremely difficult due to the non-linearity nature in the problem. Therefore, a lot of research has been done to develop an existing electrospinning simulation for viscoelastic liquids.³³

BASICS OF ELECTROSPINNING MODELING

The balance of the producing accumulation is, particularly, a basic source of the quantitative models of phenomena or processes. Differential balance equations are formulated for momentum, mass and energy through the contribution of local rates of transport expressed by the principles of Newton's, Fick's and Fourier's laws. For describing more complex systems, like electrospinning, which involves strong turbulence of the fluid flow, the characterization of the product's properties is necessary and various balances are required.³⁴

The basic principle used in modeling of the chemical engineering process is the concept of balance of momentum, mass and energy, which can be expressed in a general form as:

$$A = I + G - O - C \quad (1)$$

where: A – accumulation built up within the system; I – input entering through the system surface; G – generation produced in system volume; O – output leaving through system boundary; C – consumption used in system volume. The form of the expression depends on the level of the process phenomenon description.³⁴⁻³⁵

According to the electrospinning models, the jet dynamics is governed by a set of three equations representing mass, energy and momentum conservation for the electrically charged jet.³⁶

Mass conservation

The concept of mass conservation is widely used in many fields, such as chemistry, mechanics, and fluid dynamics. Historically, mass conservation was discovered in chemical reactions by Antoine Lavoisier in the late 18th century and was of decisive importance in the

progress from alchemy to the modern natural science of chemistry. The concept of matter conservation is useful and sufficiently accurate for most chemical calculations, even in modern practice.³⁷

The conservation laws equations that govern the fluid jet motion in the electrospinning procedure are conservation of mass and conservation of charge.³⁸

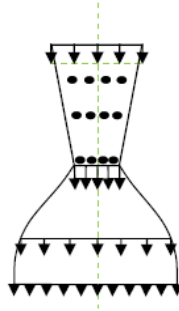


Figure 2: Macromolecular chains are compacted during electrospinning

According to the conservation of mass equation:

$$\pi R^2 v = Q \quad (2)$$

For incompressible jets, by increasing the velocity, the radius of the jet decreases, so that at the maximum level of velocity, the jet radius becomes minimum. The macromolecules of the polymers are compacted closer together, while the jet becomes thinner, as shown in Fig. 2. When the radius of the jet reaches the minimum value and its speed becomes maximum to keep the conservation of mass equation, the jet dilates by decreasing its density, which is called electrospinning dilation.³⁹⁻⁴⁰

Electric charge conservation

An electric current is a flow of electric charge, which streams in the presence of voltage across a conductor. In physics, charge conservation is the principle according to which electric charge can be neither created, nor destroyed. The net quantity of electric charge, the amount of positive charge minus the amount of negative charge in the universe, is always conserved. The first written statement of the principle was made by American scientist and statesman Benjamin Franklin in 1747. Charge conservation is a physical law that states that the amount of electric charge in any volume of space is exactly equal to the amount of charge in a region and the flow of charge into and out of that region.⁴¹

During the electrospinning process, the electrostatic repulsion between excess charges in

the solution stretches the jet. In addition, this stretching decreases the jet diameter and this fact leads to the law of charge conservation as the second governing equation.⁴²

During the electrospinning process, the electric current induced by the electric field includes both conduction and convection.

The conventional symbol for current is I :

$$I = I_{conduction} + I_{convection} \quad (3)$$

Electrical conduction is the movement of electrically charged particles through a transmission medium. This movement can form an electric current in response to an electric field. The underlying mechanism of this electric charge movement depends on the type of the materials.

$$I_{conduction} = J_{cond} \times S = KE \times \pi R^2 \quad (4)$$

$$J = \frac{I}{A(s)} \quad (5)$$

$$I = J \times S \quad (6)$$

Convection current is the flow of current in the absence of an electric field, which can be defined as:

$$I_{convection} = J_{conv} \times S = 2\pi R(L) \times \sigma v \quad (7)$$

$$J_{conv} = \sigma v \quad (8)$$

So, the total current can be calculated as:

$$\pi R^2 KE + 2\pi R v \sigma = I \quad (9)$$

Momentum balance

In classical mechanics, linear momentum or translational momentum is the mass and velocity

production of an object. Like velocity, linear momentum is a vector quantity, possessing a direction as well as a magnitude:

$$P = m v \tag{10}$$

Linear momentum is also a conserved quantity, meaning that if a closed system (one that does not exchange any matter with the outside and is not acted on by outside forces) is not affected by external forces, its total linear momentum cannot change. In classical mechanics, conservation of linear momentum is implied by Newton's laws of motion; but it also holds in special relativity (with a modified formula) and, with appropriate definitions, a (generalized) linear momentum conservation law holds in electrodynamics, quantum mechanics, quantum field theory, and general relativity.^{35, 43}

For example, according to the third law, the forces between two particles are equal and opposite. If the particles are numbered 1 and 2, the second law states:

$$F_1 = \frac{dP_1}{dt} \tag{11}$$

$$F_2 = \frac{dP_2}{dt} \tag{12}$$

Therefore:

$$\frac{dP_1}{dt} = -\frac{dP_2}{dt} \tag{13}$$

$$\frac{d}{dt}(P_1 + P_2) = 0 \tag{14}$$

If the velocities of the particles are v_{11} and v_{12} before the interaction, and afterwards they are v_{21} and v_{22} , then:

$$m_1 v_{11} + m_2 v_{12} = m_1 v_{21} + m_2 v_{22} \tag{15}$$

This law holds no matter how complicated the force is between the particles. Similarly, if there are several particles, the momentum exchanged between each pair of particles adds up to zero, as a result, the total change in momentum is zero. This conservation law applies to all interactions, including collisions and separations caused by explosive forces. It can also be generalized to situations where Newton's laws do not hold, for example in the theory of relativity and in electrodynamics.⁴³⁻⁴⁵

The momentum equation for electrospinning modeling is formulated by considering the forces on a short segment of the jet.⁴⁶⁻⁴⁷

$$\frac{d}{dz}(\pi R^2 \rho v^2) = \pi R^2 \rho g + \frac{d}{dz}[\pi R^2 (-p + \tau_{zz})] + \frac{\gamma}{R} \cdot 2\pi R R' + 2\pi R (t_i^e - t_n^e R')$$

As shown in Fig. 3, the element's angles could be defined as α and β . According to the mathematical relationships, it is obvious that:

$$\alpha + \beta = \pi / 2 \tag{17}$$

$$\sin \alpha = \tan \alpha \tag{18}$$

$$\cos \alpha = 1$$

In accordance with Figure 3, the relationships between these electric forces are as indicated below:

$$t_n^e \sin \alpha \cong t_n^e \tan \alpha \cong -t_n^e \tan \beta \cong -\frac{dR}{dz} t_n^e = -R' t_n^e \tag{19}$$

$$t_i^e \cos \alpha \cong t_i^e \tag{20}$$

So, the effect of the electric forces in the momentum balance equation can be presented as:

$$2\pi R L (t_i^e - R' t_n^e) dz \tag{21}$$

(Notation: In the main momentum equation, the final formula is obtained by dividing into dz).

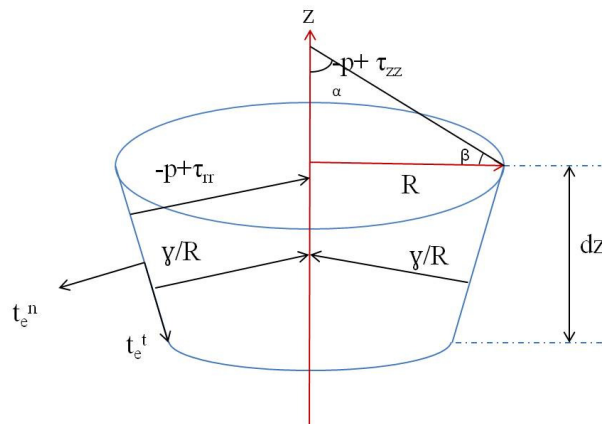


Figure 3: Momentum balance on a short section of the jet

Generally, the normal electric force is defined as:

$$t_n^e \cong \frac{1}{2} \bar{\epsilon} E_n^2 = \frac{1}{2} \bar{\epsilon} \left(\frac{\sigma}{\bar{\epsilon}} \right)^2 = \frac{\sigma^2}{2\bar{\epsilon}} \quad (22)$$

$$E_n = \frac{\sigma}{\bar{\epsilon}} \quad (23)$$

The electric force can be represented by:

$$F = \frac{\Delta W_e}{\Delta l} = \frac{1}{2} (\epsilon - \bar{\epsilon}) E^2 \times \Delta S \quad (24)$$

The force per surface unit is:

$$\frac{F}{\Delta S} = \frac{1}{2} (\epsilon - \bar{\epsilon}) E^2 \quad (25)$$

Generally the electric potential energy is obtained by:

$$U_e = -W_e = -\int F \cdot ds \quad (26)$$

$$\Delta W_e = \frac{1}{2} (\epsilon - \bar{\epsilon}) E^2 \times \Delta V = \frac{1}{2} (\epsilon - \bar{\epsilon}) E^2 \times \Delta S \cdot \Delta l \quad (27)$$

Finally, the following relationship results:

$$t_n^e = \frac{\sigma^2}{2\bar{\epsilon}} - \frac{1}{2} (\epsilon - \bar{\epsilon}) E^2 \quad (28)$$

$$t_t^e = \sigma E \quad (29)$$

Coulomb's law

Coulomb's law is a mathematical description of the electric force between charged objects, which was formulated by the 18th century French physicist Charles-Augustin de Coulomb. It is analogous to Isaac Newton's law of gravity. Both gravitational and electric forces decrease with the square of the distance between the objects, and both forces act along a line between them.⁴⁸ In Coulomb's law, the magnitude and sign of the electric force are determined by the electric charge, more than the mass of an object. Thus, charge which is a basic property matter determines how electromagnetism affects the motion of charged targets.⁴¹

Coulomb's force is thought to be the main cause for the instability of the jet in the electrospinning process.⁴⁹ This statement is based on the Earnshaw theorem, named after Samuel Earnshaw,⁵⁰ which claims that "A charged body placed in an electric field of force cannot rest in stable equilibrium under the influence of the electric forces alone". This theorem can be notably adapted to the electrospinning process.⁴⁹ The instability of a charged jet influences jet deposition and, as a consequence, nanofiber formation. Therefore, some researchers applied the developed models to the analysis of

mechanisms of jet deposition and alignment on various collecting devices in arbitrary electric fields.⁵¹

The equation for the potential along the centerline of the jet can be derived from Coulomb's law. Polarized charge density is obtained:

$$\rho_{P'} = -\bar{\nabla} \cdot \bar{P}' \quad (30)$$

Where P' is polarization:

$$\bar{P}' = (\epsilon - \bar{\epsilon}) \bar{E} \quad (31)$$

Substituting P' in equation (30), yields:

$$\rho_{P'} = -(\bar{\epsilon} - \epsilon) \frac{dE}{dz'} \quad (32)$$

Beneficial charge per surface unit can be calculated as below:

$$\rho_{P'} = \frac{Q_b}{\pi R^2} \quad (33)$$

$$Q_b = \rho_b \cdot \pi R^2 = -(\bar{\epsilon} - \epsilon) \pi R^2 \frac{dE}{dz'} \quad (34)$$

$$Q_b = -(\bar{\epsilon} - \epsilon) \pi \frac{d(ER^2)}{dz'} \quad (35)$$

$$\rho_{sb} = Q_b \cdot dz' = -(\bar{\epsilon} - \epsilon) \pi \frac{d(ER^2)}{dz'} dz' \quad (36)$$

The main equation of Coulomb's law:

$$F = \frac{1}{4\pi\epsilon_0} \frac{qq_0}{r^2} \quad (37)$$

The electric field is:

$$E = \frac{1}{4\pi\epsilon_0} \frac{q}{r^2} \quad (38)$$

The electric potential may be expressed by:

$$\Delta V = -\int E \cdot dL \quad (39)$$

$$V = \frac{1}{4\pi\epsilon_0} \frac{Q_b}{r} \quad (40)$$

According to the beneficial charge equation, the electric potential could be rewritten as:

$$\Delta V = Q(z) - Q_\infty(z) = \frac{1}{4\pi\bar{\epsilon}} \int \frac{(q - Q_b)}{r} dz' \quad (41)$$

$$Q(z) = Q_\infty(z) + \frac{1}{4\pi\bar{\epsilon}} \int \frac{q}{r} dz' - \frac{1}{4\pi\bar{\epsilon}} \int \frac{Q_b}{r} dz' \quad (42)$$

$$Q_b = -(\bar{\epsilon} - \epsilon) \pi \frac{d(ER^2)}{dz'} \quad (43)$$

In the above equations, Q and Q_∞ are the potential along the centerline of the jet and the potential due to the external field in the absence of the jet, respectively. The surface charge density's equation can be defined by:

$$q = \sigma \cdot 2\pi RL \quad (44)$$

$$r^2 = R^2 + (z - z')^2 \quad (45)$$

$$r = \sqrt{R^2 + (z - z')^2} \quad (46)$$

The final equation obtained by substituting the mentioned equations is:

$$Q(z) = Q_\infty(z) + \frac{1}{4\pi\bar{\epsilon}} \int \frac{\sigma \cdot 2\pi R}{\sqrt{(z - z')^2 + R^2}} dz' - \frac{1}{4\pi\bar{\epsilon}} \int \frac{(\bar{\epsilon} - \epsilon)\pi}{\sqrt{(z - z')^2 + R^2}} \frac{d(ER^2)}{dz'} \quad (47)$$

It is assumed that the dielectric constant ratio, which is represented by β , is defined as:

$$\beta = \frac{\epsilon}{\bar{\epsilon}} - 1 = -\frac{(\bar{\epsilon} - \epsilon)}{\bar{\epsilon}} \quad (48)$$

So, now the potential along the centerline of the jet, due to the total surface charges may be obtained by:

$$Q(z) = Q_\infty(z) + \frac{1}{2\bar{\epsilon}} \int \frac{\sigma R}{\sqrt{(z - z')^2 + R^2}} dz' - \frac{\beta}{4} \int \frac{1}{\sqrt{(z - z')^2 + R^2}} \frac{d(ER^2)}{dz'} \quad (49)$$

The asymptotic approximation of χ is used to evaluate the integrals mentioned above:

$$\chi = \left(-z + \xi + \sqrt{z^2 - 2z\xi + \xi^2 + R^2} \right) \quad (50)$$

where χ is "aspect ratio" of the jet (L = length, R_0 = Initial radius)

This leads to the final relation for the axial electric field:

$$E(z) = E_\infty(z) - \ln \chi \left(\frac{1}{\bar{\epsilon}} \frac{d(\sigma R)}{dz} - \frac{\beta}{2} \frac{d^2(ER^2)}{dz^2} \right) \quad (51)$$

Constitutive equations

In modern condensed matter physics, the constitutive equation plays a major role. In physics and engineering, a constitutive equation or relation is the relation between two physical quantities that is specific to a material or substance, and approximates the response of that material to an external stimulus, usually as applied fields or forces.⁵² There is a sort of mechanical equation of state, which describes how the material is constituted mechanically. With these constitutive relations, the vital role of the material is reasserted.⁵³ There are two groups of constitutive equations: linear and nonlinear constitutive equations.⁵⁴ These equations are combined with other governing physical laws to solve problems; for example in fluid mechanics the flow of a fluid in a pipe, in solid state physics the response of a crystal to an electric field, or in structural analysis the connection between applied stresses or forces to strains or deformations can be considered as constitutive relations.⁵²

The first constitutive equation (constitutive law) was developed by Robert Hooke and is known as Hooke's law. It deals with the case of linear elastic materials. Following this discovery, this type of equation, often called a "stress-strain relation" in this example, but also called a "constitutive assumption" or an "equation of

state" was commonly used.⁵⁵ Walter Noll advanced the use of constitutive equations, clarifying their classification and the role of invariance requirements, constraints, and definitions of terms like "material", "isotropic", "aeolotropic", etc. The class of "constitutive relations" of the form stress rate (velocity gradient, stress, density) was the subject of Walter Noll's dissertation in 1954 under Clifford Truesdell.⁵² There are several kinds of constitutive equations that are commonly applied in electrospinning. Some of these applicable equations are discussed below.

Ostwald–de Waele power law

The rheological behavior of many polymeric fluids can be described by power law constitutive equations.⁵⁴ The equations that describe the dynamics in electrospinning constitute, at a minimum, those describing the conservation of mass, momentum and charge, and the electric field equation. Additionally, a constitutive equation for the fluid behavior is also required.⁵⁶ A Power-law fluid, or the Ostwald–de Waele relationship, is a type of generalized Newtonian fluid for which the shear stress, τ , is given by:

$$\tau = K \left(\frac{\partial v}{\partial y} \right)^m \quad (52)$$

Which $\partial v/\partial y$ is the shear rate or the velocity gradient perpendicular to the plane of shear. The power law is only a good description of fluid behavior across the range of shear rates to which the coefficients are fitted. There are other models that better describe the entire flow behavior of shear-dependent fluids, but they don't have enough simplicity, so the power law is still used to describe fluid behavior, permit mathematical predictions, and correlate experimental data.^{47, 57}

Nonlinear rheological constitutive equations applicable for polymer fluids (Ostwald–de Waele power law) were applied to the electrospinning process by Spivak and Dzenis.⁵⁸⁻⁶⁰

$$\hat{\tau}^c = \mu \left[\text{tr}(\dot{\gamma}^2) \right]^{(m-1)/2} \dot{\gamma} \quad (53)$$

$$\mu = K \left(\frac{\partial v}{\partial y} \right)^{m-1} \quad (54)$$

Viscous Newtonian fluids are described by a special case of the above equation with the flow index of $m = 1$. Pseudoplastic (shear thinning) fluids are described by flow indices in the range of $0 \leq m \leq 1$ and dilatant (shear thickening) fluids are described by the those of $m > 1$.⁵⁹

Giesekus equation

In 1966, Giesekus established the concept of anisotropic forces and motions in polymer kinetic theory. With particular choices for the tensors describing the anisotropy, one could obtain the Giesekus constitutive equation from the elastic dumbbell kinetic theory.⁶¹⁻⁶² The Giesekus equation is known to predict, both qualitatively and quantitatively, material functions for steady and non-steady shear and elongational flows. However, the equation has two significant drawbacks: it predicts that the viscosity is inversely proportional to the shear rate in the limit of infinite shear rate and it is unable to predict any decrease in the elongational viscosity with increasing elongation rate in uniaxial elongational flow. The first one is not serious because of retardation time, which is included in the constitutive equation, but the latter is more critical because the elongational viscosity of some polymers decreases with the increase of elongation rate.⁶³⁻⁶⁴

In the main Giesekus equation, the tensor of excess stresses depending on the motion of polymer units relative to their surroundings was connected to a sequence of tensors characterizing the configuration state of the different kinds of

network structures present in the concentrated solution or melt. The respective set of constitutive equations indicates:⁶⁵⁻⁶⁶

$$S_k + \eta \frac{\partial C_k}{\partial t} = 0 \quad (55)$$

The equation below indicates the upper convected time derivative (Oldroyd derivative):

$$\frac{\partial C_k}{\partial t} = \frac{DC_k}{Dt} - [C_k \nabla v + (\nabla v)^T C_k] \quad (56)$$

(Note: The upper convective derivative is the rate of change of some tensor property of a small parcel of fluid that is written in the coordinate system rotating and stretching with the fluid.)

C_k can also be measured as:

$$C_k = 1 + 2E_k \quad (57)$$

According to the concept of “recoverable strain” S_k may be understood as a function of E_k and vice versa. The linear relations corresponding to Hooke's law are indicated as:

$$S_k = 2\mu_k E_k \quad (58)$$

So:

$$S_k = \mu_k (C_k - 1) \quad (59)$$

Equation (55) becomes:

$$S_k + \lambda_k \frac{\partial S_k}{\partial t} = 2\eta D \quad (60)$$

$$\lambda_k = \frac{\eta}{\mu_k} \quad (61)$$

As a second step, the scalar mobility constant B_k (which is contained in the constants η) can be used to simplify the model as below:

$$\frac{1}{2}(\beta_k S_k + S_k \beta_k) + \tilde{\eta} \frac{\partial C_k}{\partial t} = 0 \quad (62)$$

The two parts of equation (62) are reduced to the single constitutive equation below:

$$\beta_k + \tilde{\eta} \frac{\partial C_k}{\partial t} = 0 \quad (63)$$

The excess tension tensor in the deformed network structure, where the well-known constitutive equation of a so-called Neo-Hookean material is proposed, might be expressed as:^{65, 67}

$$\left\{ \begin{array}{l} \text{Neo-Hookean equation:} \\ S_k = 2\mu_k E_k = \mu_k (C_k - 1) \end{array} \right. \quad (64)$$

$$\left\{ \begin{array}{l} \mu_k = NKT \\ \beta_k = 1 + \alpha(C_k - 1) = (1 - \alpha) + \alpha C_k \end{array} \right. \quad (65)$$

where K is Boltzmann's constant.

By substitution of equations (64) and (65) in equation (61), a relation could be obtained where the condition $0 \leq \alpha \leq 1$ must be fulfilled due to

the limiting case $\alpha = 0$, which corresponds to an isotropic mobility.⁶⁸

$$\left\{ \begin{array}{l} 0 \leq \alpha \leq 1 \\ \alpha = 1 \\ 0 \leq \alpha \leq 1 \end{array} \right. \quad [1 + \alpha(C_k - 1)]C_k - 1 + \lambda_k \frac{\partial C_k}{\partial t} = 0 \quad (66)$$

$$C_k(C_k - 1) + \lambda_k \frac{\partial C_k}{\partial t} = 0 \quad (67)$$

$$C_k = \frac{S_k}{\mu_k} + 1 \quad (68)$$

Substituting the equations above in equation (61) yields:

$$\left[1 + \frac{\alpha S_k}{\mu_k} \right] \frac{S_k}{\mu_k} + \lambda_k \frac{\partial C_k}{\partial t} = 0 \quad (69)$$

$$\frac{S_k}{\mu_k} + \frac{\alpha S_k^2}{\mu_k^2} + \lambda_k \frac{\partial (S_k / \mu_k + 1)}{\partial t} = 0 \quad (70)$$

$$\frac{S_k}{\mu_k} + \frac{\alpha S_k^2}{\mu_k^2} + \frac{\lambda_k}{\mu_k} \frac{\partial S_k}{\partial t} = 0 \quad (71)$$

$$S_k + \frac{\alpha S_k^2}{\mu_k} + \lambda_k \frac{\partial S_k}{\partial t} = 0 \quad (72)$$

Symbol D refers to the rate of strain tensor of the material continuum.⁶⁵

$$D = \frac{1}{2} [\nabla v + (\nabla v)^T] \quad (73)$$

The equation of the upper convected time derivative for all fluid properties can be calculated as:

$$\frac{\partial \otimes}{\partial t} = \frac{D \otimes}{Dt} - [\otimes \cdot \nabla v + (\nabla v)^T \cdot \otimes] \quad (74)$$

$$\frac{D \otimes}{Dt} = \frac{\partial \otimes}{\partial t} + [(v \cdot \nabla) \cdot \otimes] \quad (75)$$

By replacing the symbol with S_k (76):

$$\lambda_k \frac{\partial S_k}{\partial t} = \lambda_k \frac{DS_k}{Dt} - \lambda_k [S_k \cdot \nabla v + (\nabla v)^T \cdot S_k] = \lambda_k \frac{DS_k}{Dt} - \lambda_k (v \cdot \nabla) S_k$$

Simplifying the equation above:

$$S_k + \frac{\alpha S_k^2}{\mu_k} + \lambda_k \frac{DS_k}{Dt} = \lambda_k (v \cdot \nabla) S_k \quad (77)$$

$$S_k = 2\mu_k E_k \quad (78)$$

The assumption of $E_k = 1$ would lead to the following equation:

$$S_k + \frac{\alpha \lambda_k S_k^2}{\eta} + \lambda_k \frac{DS_k}{Dt} = \frac{\eta}{\mu_k} (2\mu_k) D = 2\eta D = \eta [\nabla v + (\nabla v)^T] \quad (79)$$

In electrospinning modeling article τ is commonly used instead of S_k .^{36, 39, 69}

$$S_k \leftrightarrow \tau$$

$$\tau + \frac{\alpha \lambda_k \tau^2}{\eta} + \lambda_k \tau_{(1)} = \eta [\nabla v + (\nabla v)^T] \quad (80)$$

Maxwell equation

Maxwell's equations are a set of partial differential equations, which, together with the Lorentz force law, form the foundation of classical electrodynamics, classical optics, and electric circuits. These fields are the bases of modern electrical and communications technologies. Maxwell's equations describe how electric and magnetic fields are generated and altered by each other and by charges and currents. They are named after the Scottish physicist and mathematician James Clerk Maxwell, who published an early form of those equations between 1861 and 1862.⁷⁰⁻⁷¹

The simplest model of flexible macromolecules in a dilute solution is the elastic dumbbell (or bead-spring) model. This has been widely used for purely mechanical theories of the stress in electrospinning modeling.⁷²

A Maxwell constitutive equation was first applied by Reneker *et al.* in 2000. Consider an electrified liquid jet in an electric field parallel to its axis. They modeled a segment of the jet by a viscoelastic dumbbell. They used a Gaussian electrostatic system of units. According to this model, each particle in the electric field exerts repulsive force on another particle. Therefore, the stress between these particles can be measured by:⁵¹

$$\frac{d\sigma}{dt} = G \frac{dl}{dt} - \frac{G}{\eta} \sigma \quad (81)$$

The stress can be calculated by a Maxwell viscoelastic constitutive equation:⁷³

$$\dot{\tau} = G \left(\epsilon' - \frac{\tau}{\eta} \right) \quad (82)$$

Where ϵ' is the Lagrangian axial strain:

$$\epsilon' \equiv \frac{\partial \dot{x}}{\partial \xi} \hat{t} \quad (83)$$

Scaling

The physical aspect of a phenomenon can apply the language of differential equation, which represents the system structure by selecting the characterizing variables and a certain mathematical constraint on the values of those variables can be accepted. These equations can predict the behavior of the system over a quantity as time; for instance, a set of continuous functions

of time that describe the way in which the system variables developed over time starting from a given initial state.⁷⁴ In general, the renormalization group theory, scaling and fractal geometry, are applied to understand complex phenomena in physics, economics and medicine.⁷⁵

In the last decade, statistical mechanics claimed that the expression "scaling laws" referred to the homogeneity form of the thermodynamic and correlation functions near the critical points, and to the resulting relations among the exponents occurring in those functions. From the viewpoint of scaling, electrospinning modeling can be studied in two ways, by allometric and dimensionless analyses. Scaling and dimensional analyses actually started with Newton, and allometry exists everywhere in our daily life and scientific activity.⁷⁵⁻⁷⁶

Allometric scaling

Electrospinning applies electrically generated motion to spin fibers. So, it is difficult to predict the size of the produced fibers, which depends on the applied voltage in principal. Therefore, the relationship between the radius of the jet and the axial distance from the nozzle is always the subject of investigations.⁷⁷⁻⁷⁸ It can be described as an allometric equation by using the values of the scaling exponent for the initial steady, instability and terminal stages.⁷⁹

The relationship between r and z can be expressed as an allometric equation in the form of:

$$r \approx z^b \quad (84)$$

When the power exponent $b = 1$, the relationship is isometric and when $b \neq 1$, the relationship is allometric.^{78, 80} From another point of view, $b = -1/2$ is considered for the straight jet, $b = -1/4$ for the instability jet and $b = 0$ for the final stage.^{54, 77}

Due to the high electrical force acting on the jet, it can be illustrated as:⁷⁸

$$\frac{d}{dz} \left(\frac{v^2}{2} \right) = \frac{2\sigma E}{\rho r} \quad (85)$$

The equations of mass and charge conservations are applied here as mentioned before.^{78, 80-81}

From the above equations, it can be remarked that (86):^{39, 78}

$$v \approx r^{-2}, \sigma \approx r, E \approx r^{-2}, \frac{dv^2}{dz} \approx r^{-2}, r \approx z^{-1/2}$$

The charged jet can be considered as a one-dimensional flow, as mentioned earlier. If the conservation equations are modified, they change as:⁷⁸

$$2\pi r \sigma^\alpha v + K\pi^2 E = I \quad (87)$$

$$r \approx z^{-\frac{\alpha}{\alpha+1}} \quad (88)$$

where α is a surface charge parameter, the value of α depends on the surface charge in the jet. When $\alpha = 0$, there is no charge in the jet surface, and when $\alpha = 1$, there is full surface charge.

Allometric scaling equations are more widely investigated by different researchers. Some of the most important allometric relationships for electrospinning are presented in Table 2.

Table 2
Investigated scaling laws applied in the electrospinning model

| Ref. | Equation | Parameters |
|------|---|--|
| 39 | $g \approx c^\beta$ | Conductance and polymer concentration |
| 77 | $d \approx \eta^\alpha$ | Fiber diameters and solution viscosity |
| 79 | $\bar{\sigma} \approx E_{\text{threshold}}^{-\alpha}$ | Mechanical strength and threshold voltage |
| 79 | $E_{\text{threshold}} \approx \eta^{1/4}$ | Threshold voltage and solution viscosity |
| 79 | $\eta \approx \omega^{-0.4}$ | Viscosity and oscillating frequency |
| 81 | $I \approx Q^b$ | Volume flow rate and current |
| 82 | $I \approx r^2$ | Current and fiber radius |
| 82 | $\sigma \approx r^3$ | Surface charge density and fiber radius |
| 82 | $\phi \approx r^2$ | Induction surface current and fiber radius |
| 54 | $r \approx \Omega^{1/4}$ | Fiber radius and AC frequency |

β , α and b = scaling exponents

Dimensionless analysis

One of the simplest, yet most powerful tools in physics is dimensional analysis, in which there are two kinds of quantities: dimensionless and dimensional. Dimensionless quantities, which have no associated physical dimensions, are widely used in mathematics, physics, engineering, economics, and in everyday life (such as in counting). Numerous well-known quantities, such as π , e , and ϕ , are dimensionless. They are "pure" numbers, and as such always have a dimension of 1.⁸³⁻⁸⁴

Dimensionless quantities are often defined as products or ratios of quantities that are not dimensionless, but whose dimensions cancel out when their powers are multiplied.⁸⁵

In non-dimensional scaling, there are two key steps:

- (a) Identifying a set of physically relevant dimensionless groups, and
- (b) Determining the scaling exponent for each one.

Dimensional analysis will help with step (a), but it cannot be possibly applicable for step (b).

A good approach to systematically getting to grips with such problems is through the tools of dimensional analysis. The dominant balance of forces controlling the dynamics of any process depends on the relative magnitudes of each underlying physical effect entering the set of governing equations.⁸⁶ The most general characteristic parameters used in dimensionless analysis in electrospinning are introduced in Table 3.

For achieving a simplified form of the equations and reducing the number of unknown variables, the parameters should be subdivided into characteristic scales in order to become dimensionless. Electrospinning dimensionless groups are shown in Table 4.⁸⁷

The governing and constitutive equations can be transformed into a dimensionless form, using the dimensionless parameters and groups.

Table 3
Characteristic parameters employed and their definitions

| Definition | Parameter |
|-----------------------------------|------------------------|
| R_0 | Length |
| $v_0 = \frac{Q}{\pi R_0^2 K}$ | Velocity |
| $E_0 = \frac{I}{\pi R_0^2 K}$ | Electric field |
| $\sigma_0 = \bar{\epsilon} E_0$ | Surface charge density |
| $\tau_0 = \frac{\eta_0 v_0}{R_0}$ | Viscous stress |

Table 4
Dimensionless groups employed and their definitions

| Field of application | Definition | Name |
|---|---|------------------------|
| Ratio of inertial to gravitational forces | $Fr = \frac{v_0^2}{gR_0}$ | Froude number |
| Ratio of inertia forces to viscous forces | $Re = \frac{\rho v_0 R_0}{\eta_0}$ | Reynolds number |
| Ratio of surface tension forces to inertia forces | $We = \frac{\rho v_0^2 R_0}{\gamma}$ | Weber number |
| Ratio of fluid relaxation time to instability growth time | $De = \frac{\lambda v_0}{R_0}$ | Deborah number |
| Ratio of characteristic time for flow to that for electrical conduction | $Pe = \frac{2\bar{\epsilon} v_0}{KR_0}$ | Electric Peclet number |

| | | |
|---|--|-------------------------------|
| Ratio of electrostatic forces to inertia forces | $Eu = \frac{\epsilon_0 E^2}{\rho v_0^2}$ | Euler number |
| Ratio of inertia forces to viscous forces | $Ca = \frac{\eta v_0}{\gamma}$ | Capillary number |
| Ratio of viscous force to surface force | $oh = \frac{\eta}{(\rho \gamma R_0)^{1/2}}$ | Ohnesorge number |
| Ratio of polymer viscosity to total viscosity | $r_\eta = \frac{\eta_p}{\eta_0}$ | Viscosity ratio |
| Ratio of length to primary radius of jet | $\chi = \frac{L}{R_0}$ | Aspect ratio |
| Relative importance of electrostatic and hydrodynamic forces | $\epsilon = \frac{\bar{\epsilon} E_0^2}{\rho v_0^2}$ | Electrostatic force parameter |
| Ratio of the electric permittivity of a substance to the permittivity of free space | $\beta = \frac{\epsilon}{\bar{\epsilon}} - 1$ | Dielectric constant ratio |

SOME ELECTROSPINNING MODELS

The most important mathematical models for the electrospinning process are classified in Table 5, according to the year, advantages and

disadvantages of the models. The most frequent numeric mathematical methods, which were used in different models, are listed in Table 6.

Table 5
The most important mathematical models for electrospinning

| Ref. | Year | Model | Researchers |
|------|------|---|---------------------------------|
| 88 | 1969 | Leaky dielectric model | Taylor, G. I. Melcher, J. R. |
| | | ✓ Dielectric fluid | |
| | | ✓ Bulk charge in the fluid jet considered to be zero | |
| | | ✓ Only axial motion | |
| | | ✓ Steady state part of jet | |
| 89 | 1996 | Slender body | Ramos |
| | | ✓ Incompressible and axi-symmetric and viscous jet under gravity force | |
| | | ✓ No electrical force | |
| | | ✓ Jet radius decreases near zero | |
| | | ✓ Velocity and pressure of jet only change during axial direction | |
| | | ✓ Mass and volume control eqs. and Taylor expansion were applied to predict jet radius | |
| 88 | 1997 | Electrohydrodynamic model | Saville, D. A. |
| | | ✓ The hydrodynamic eq. of dielectric model was modified | |
| | | ✓ Using dielectric assumption | |
| | | ✓ This model can predict drop formation | |
| | | ✓ Considering jet as a cylinder (ignoring the diameter reduction) | |
| | | ✓ Only for steady state part of the jet | |
| 59 | 1998 | Spivak & Dzenis model | Spivak, A. Dzenis, Y. |
| | | ✓ The motion of a viscose fluid jet with lower conductivity were surveyed in an external electric field | |
| | | ✓ Single Newtonian fluid jet | |
| | | ✓ The electric field assumed to be uniform and | |

| | | | |
|----|------|---|--------------------------------|
| | | <ul style="list-style-type: none"> constant, unaffected by the charges carried by the jet ✓ The asymptotic approximation was applied in a long distance from the nozzle ✓ Tangential electric force assumed to be zero ✓ By using non-linear rheological constitutive eq. (Ostwald-de Waele power law), non-linear behavior of fluid jet was investigated | |
| 90 | 2000 | <p>Droplet formation model</p> <ul style="list-style-type: none"> ✓ Droplet formation of the charged fluid jet was studied in this model ✓ The ratio of mass, energy and electric charge transition are the most important parameters on droplet formation ✓ Deformation and break-up of droplets were investigated too ✓ Newtonian and non-Newtonian fluids ✓ Only for high conductivity and viscous fluids | Jong Wook |
| 51 | 2000 | <p>Reneker model</p> <ul style="list-style-type: none"> ✓ For description of instabilities in viscoelastic jets ✓ Using molecular chain theory, behavior of polymer chain by spring-bead model in electric field was studied ✓ Electric force based on electric field cause instability of fluid jet, while repulsion force between surface charges make perturbation and bending instability ✓ The motion path of these two cases were studied ✓ Governing eqs.: momentum balance, motion eqs. for each bead, Maxwell tension and columbic eqs. | Reneker, D. H. Yarin, A. L. |
| 38 | 2001 | <p>Stability theory</p> <ul style="list-style-type: none"> ✓ This model is based on a dielectric model with some modification for Newtonian fluids ✓ This model can describe whipping, bending and Rayleigh instabilities and introduced new ballooning instability ✓ 4 motion regions were introduced: dipping mode, spindle mode, oscillating mode, precession mode. ✓ Surface charge density introduced as the most effective parameter on instability formation ✓ Effect of fluid conductivity and viscosity on nanofibers diameter were discussed ✓ Steady solutions may be obtained only if the surface charge density at the nozzle is set to zero or a very low value | Hohman, M. Shin, M. |
| 46 | 2002 | <ul style="list-style-type: none"> ✓ Modifying Hohman model ✓ For both Newtonian and non-Newtonian fluids ✓ Unlike Hohman model, the initial surface charge density was not zero, so the “ballooning instability” did not accrue ✓ Only for steady state part of the jet ✓ Simplifying the electric field equation, which Hohman used in order to eliminate Ballooning instability | Feng, J. J |

| | | | |
|----|------|---|--|
| 60 | 2004 | <p>Wan-Guo-Pan model</p> <ul style="list-style-type: none"> ✓ They introduced thermo-electro-hydro dynamics model in electrospinning process ✓ This model is a modification of Spivak's model mentioned above ✓ The governing eqs. in this model: Modified Maxwell eq., Navier-Stocks eqs., and several rheological constitutive eq. | Wan-Guo-Pan |
| 54 | 2005 | <p>AC-electrospinning model</p> <ul style="list-style-type: none"> ✓ Whipping instability in this model was distinguished as the most effective parameter on uncontrollable deposition of nanofibers ✓ Applying AC current can reduce this instability and make oriented nanofibers ✓ This model found a relationship between the axial distance from nozzle and jet diameter ✓ This model also connected AC frequency and jet diameter | Ji-Haun |
| 36 | 2007 | <p>Combination of slender body and dielectric model</p> <ul style="list-style-type: none"> ✓ This is a new model for viscoelastic jets in electrospinning, combining these two models ✓ All variables were assumed uniform in cross section of the jet, but they changed in z direction ✓ Nanofiber diameter can be predicted | Roozmond (Eindhoven University and Technology) |
| 26 | 2012 | <p>Electromagnetic model</p> <ul style="list-style-type: none"> ✓ Results indicated that the electromagnetic field formed due to the electrical field in the charged polymeric jet is the most important reason of the helix motion of the jet during the process | Wan |
| 91 | 2012 | <p>Dasri model</p> <ul style="list-style-type: none"> ✓ This model was presented for describing the unstable behavior of the fluid jet during electrospinning ✓ This instability causes random deposition of nanofiber on the surface of the collector ✓ This model described the dynamic behavior of the fluid by combining the assumptions of Reneker's and Spivak's models | Dasri |

LECTROSPINNING SIMULATION EXAMPLE

In order to survey of the application of electrospinning modeling, its main equations were applied for simulating the process according to the constants summarized in Table 6.

Mass and charge conservations allow v and σ to be expressed in terms of R and E , and the momentum and E-field equations can be recast into two second-order ordinary differential equations for R and E . The slender-body theory (the straight part of the jet) was assumed to investigate jet behavior during the spinning distance. The slope of the jet surface (R') is

maximum at the origin of the nozzle. The same assumption has been used in most previous models concerning jets or drops. The initial and boundary conditions that govern the process are introduced as:

Initial values ($z = 0$):

$$R(0) = 1$$

$$E(0) = E_0$$

$$\tau_{pr} = 2r_\eta \frac{R_0'}{R_0^3}$$

$$\tau_{pz} = -2\tau_{pr}$$

(89)

Table 6
Applied numerical methods for electrospinning

| Ref. | Method |
|------------|--|
| 35, 36, 46 | Relaxation method |
| 73, 90 | Boundary integral method (boundary element method) |
| 36, 54 | Semi-inverse method |
| 89 | (Integral) control-volume formulation |
| 88 | Finite element method |
| 92 | Kutta-Merson method |
| 42 | Lattice Boltzmann method with finite difference method |

Feng⁴⁶ indicated that E(0) effect is limited to a tiny layer below the nozzle, whose thickness is a few percent of R_0 . It was assumed that the shear inside the nozzle is effective in stretching polymer molecules, as compared with the following elongation. Boundary values can be expressed as: Boundary values ($z = \chi$):

$$\begin{aligned}
 R(\chi) + 4\chi R'(\chi) &= 0 \\
 E(\chi) &= E_\chi \\
 \tau_{pr} &= 2r_\eta \frac{R_\chi'}{R_\chi^3} \\
 \tau_{pz} &= -2\tau_{pr}
 \end{aligned} \tag{90}$$

The asymptotic scaling can be stated as:⁴⁶

$$R(z) \propto z^{-1/4} \tag{91}$$

Just above the deposit point ($z = \chi$), asymptotic thinning conditions are applied. R drops towards zero and E approaches E_∞ . The electric field is not equal to E_∞ , so we assumed a slightly larger value, E_χ .

The momentum, electric field and stress equations could be rewritten into a set of four coupled first-order ordinary differential equations (ODE's) with the above mentioned boundary conditions. The numerical relaxation method has been chosen to solve the generated boundary value problem.

The results of these systems of equations are presented in Figs. 4 and 5, and match quite well with those of other studies that have been published.^{36, 38, 46, 69, 93}

The variation prediction of R, R', ER^2 , $ER^{2'}$ and E versus axial position (z) is shown in Fig. 4. Physically, the amount of conductive charges reduces with decreasing jet radius. Therefore, to

maintain the same jet current, more surface charges should be carried by the convection.

Moreover, in the considered simulation region, the density of surface charge gradually increased. As the jet gets thinner and faster, electric conduction gradually transfers to convection. The electric field is mainly induced by the axial gradient of surface charge, thus, it is insensitive to the thinning of the electrospun jet:

$$\frac{d(\sigma R)}{dz} \approx -\left(2R \frac{dR}{dz}\right) / Pe \tag{92}$$

Therefore, the variation of E versus z can be written as:

$$\frac{d(E)}{dz} \approx \ln \chi \left(\frac{d^2 R^2}{dz^2} \right) / Pe \tag{93}$$

Downstream of the origin, E shoots up to a peak and then relaxes due to the decrease of the electrostatic pulling force in consequence of the reduction of surface charge density, if the current is held at a constant value. However, in reality, the increase of the strength of the electric field also increases the jet current, which is relatively linear.^{46, 93}

As the jet becomes thinner downstream, the increase of jet speed reduces the surface charge density and thus E, so the electric force exerted on the jet and thus R' become smaller. The rates of R and R' are maximum at $z = 0$, and then relax smoothly toward zero along the jet flow.^{36, 46} According to the relation between R, E and z, ER^2 and $ER^{2'}$ vary as shown in Fig. 4 (c) and (d).

Fig. 5 shows the changes of axial, radial shear stress and the difference between them, the tensile force (T) versus z. The polymer tensile force is much larger in viscoelastic polymers because of the strain hardening. T also has an initial rise, because the effect of strain hardening is so strong that it overcomes the shrinking radius of the jet.

Table 7
 Constants used in electrospinning simulation

| Quantity | Constant |
|----------------------|----------|
| 2.5×10^{-3} | Re |
| 0.1 | We |
| 0.1 | Fr |
| 0.1 | Pe |
| 10 | De |
| 1 | E |
| 40 | β |
| 20 | χ |
| 0.7 | E_0 |
| 0.5 | E_χ |
| 0.9 | r_η |

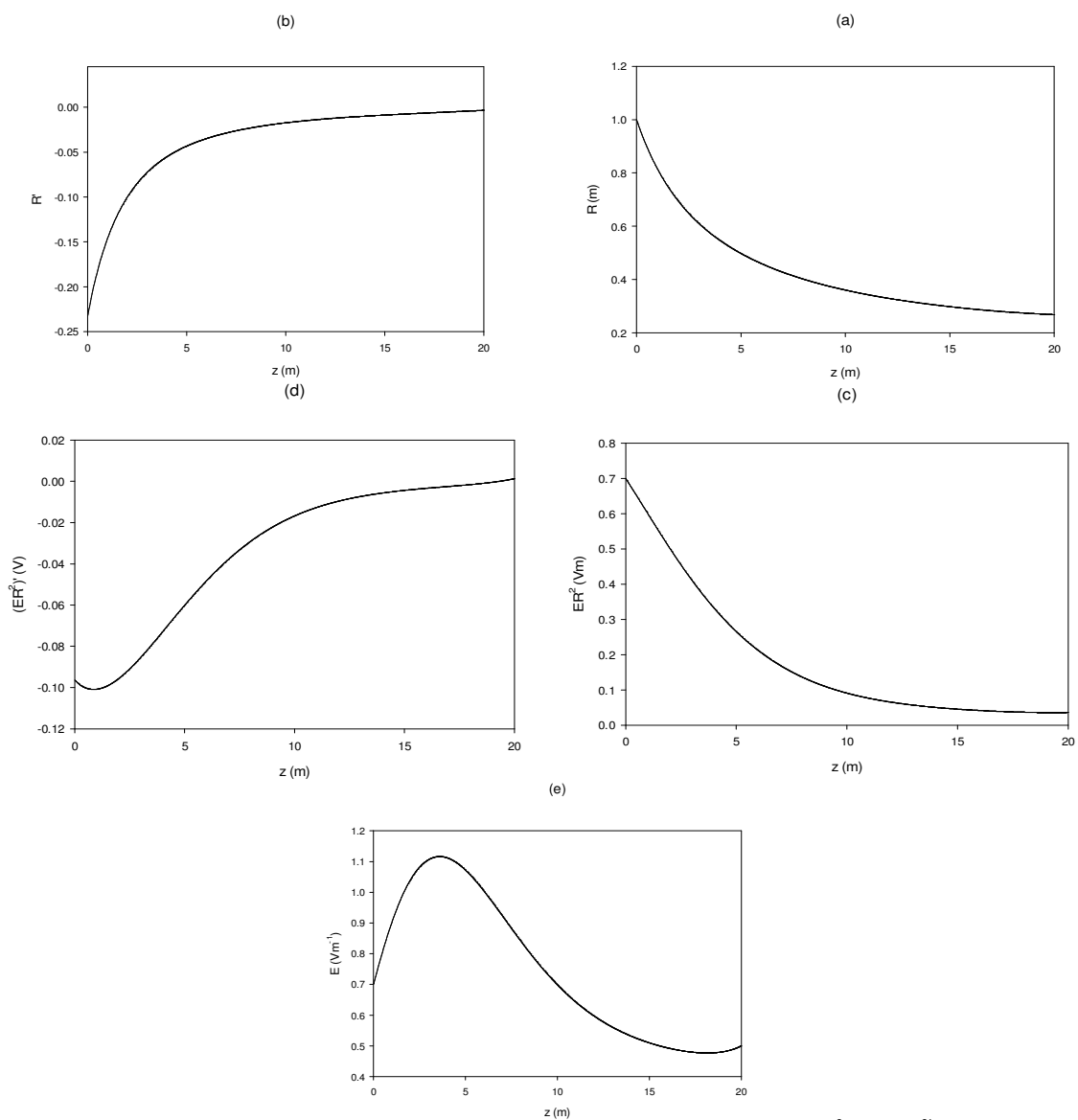


Figure 4: Solutions given by the electrospinning model for (a) R ; (b) R' ; (c) ER^2 ; (d) ER^2' and (e) E

After the maximum value of T , it reduces during the jet thinning. As expected, the axial polymer stress rises, because the fiber is stretched in axial direction, and the radial polymer stress declines. The variation of T along the jet can be nonmonotonic, however, meaning the viscous

normal stress may promote or resist stretching in a different part of the jet and under different conditions.^{36, 46} For investigating the simulation accuracy, the plots obtained by other researchers are presented in Figures 6, 7 and 8.

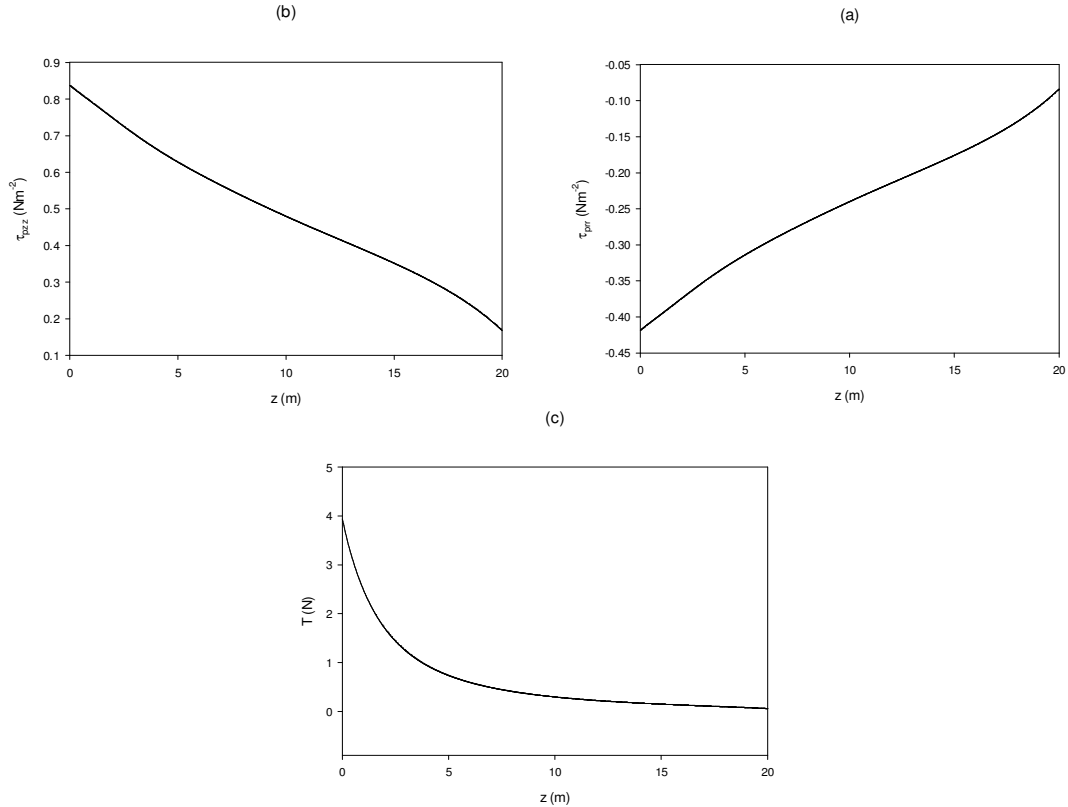


Figure 5: Solutions given by the electrospinning model for (a) τ_{prr} ; (b) τ_{pzz} and (c) T

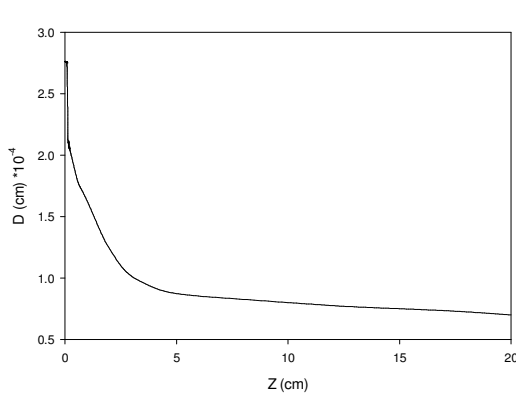


Figure 7: Relationships between jet diameter and the distance from nozzle to grounded collecting plate⁹⁵

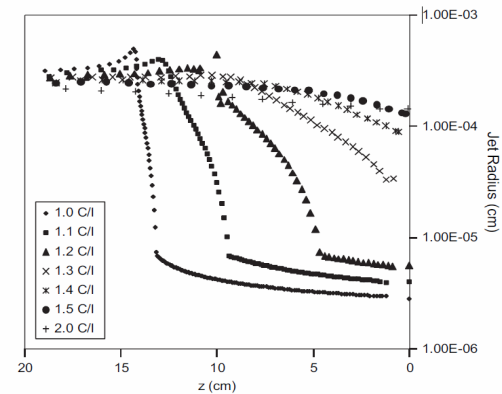


Figure 6: Distributions of jet radius (R) versus z coordinate⁹⁴

For example, Thompson *et al.* studied thirteen parameters in the electrospinning model. They showed that some parameters like volumetric charge density, distance from nozzle to collector,

initial jet radius, relaxation time, and elongational viscosity have the largest influence on the resulting electrospun fiber diameter. Five other parameters have a moderate effect and three

parameters have a minor effect. Thompson *et al.* presented the effect of the volumetric charge density of the jet radius along z direction as the most significant effective parameter.⁹⁴ In another approach, Xu *et al.* investigated a discrete mathematical model of a magnetic electrospinning process, which was used for numerical analysis of the excitation current effect on electrospinning. They showed that the simulation results agreed well with the experimental data.⁹⁵ As could be seen, the jet radius has a decreasing trend in all cases, which is in agreement with the obtained procedure in the considered simulation.

Feng employed the slender-body theory for the stretching of a straight charged jet of Giesekus fluid in his approach. He and his coworkers applied the measurement of jet radius, which was obtained in the laboratory of Doshi and Reneker

for the PEO solution and compared the results with the predicted simulation outcomes. The trend of the different parameters shown in the diagrams (Fig. 8) is similar to our results.⁶⁹

A model for electrospinning of a Newtonian fluid, which was introduced by Feng for the first time, was implemented in Fortran code based on a relaxation method and expanded to a Newtonian viscoelastic fluid, using the Giesekus constitutive equation, by Solberg *et al.* The main issue with the relaxation method was to provide the code with a sufficiently accurate initial guess. The presented method was based on a Newtonian solution as an initial guess for the viscoelastic model, then solutions for a viscoelastic and a Newtonian fluid were compared with each other.

The plots in their study presented the same proceeding as Feng's model.³⁶

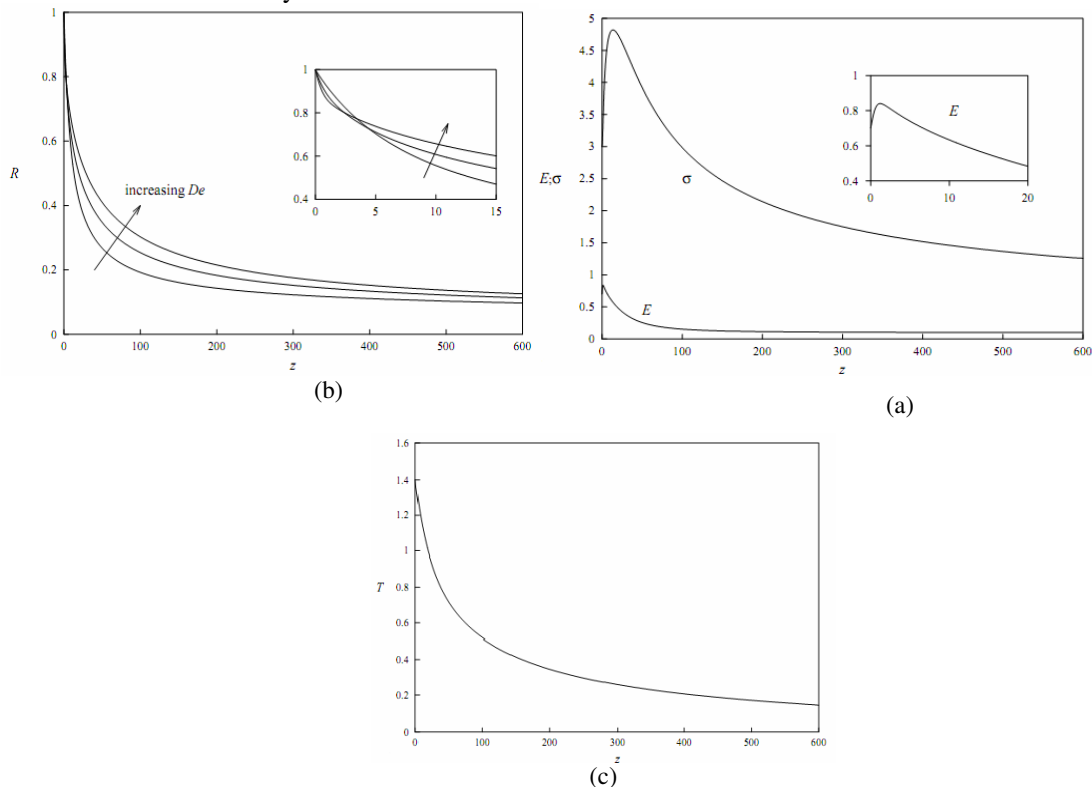


Figure 8: Deliberation on (a) R , (b) E, σ and (c) T changes versus z coordinate (inner plots were obtained by experiments and outer plots by simulation⁶⁹)

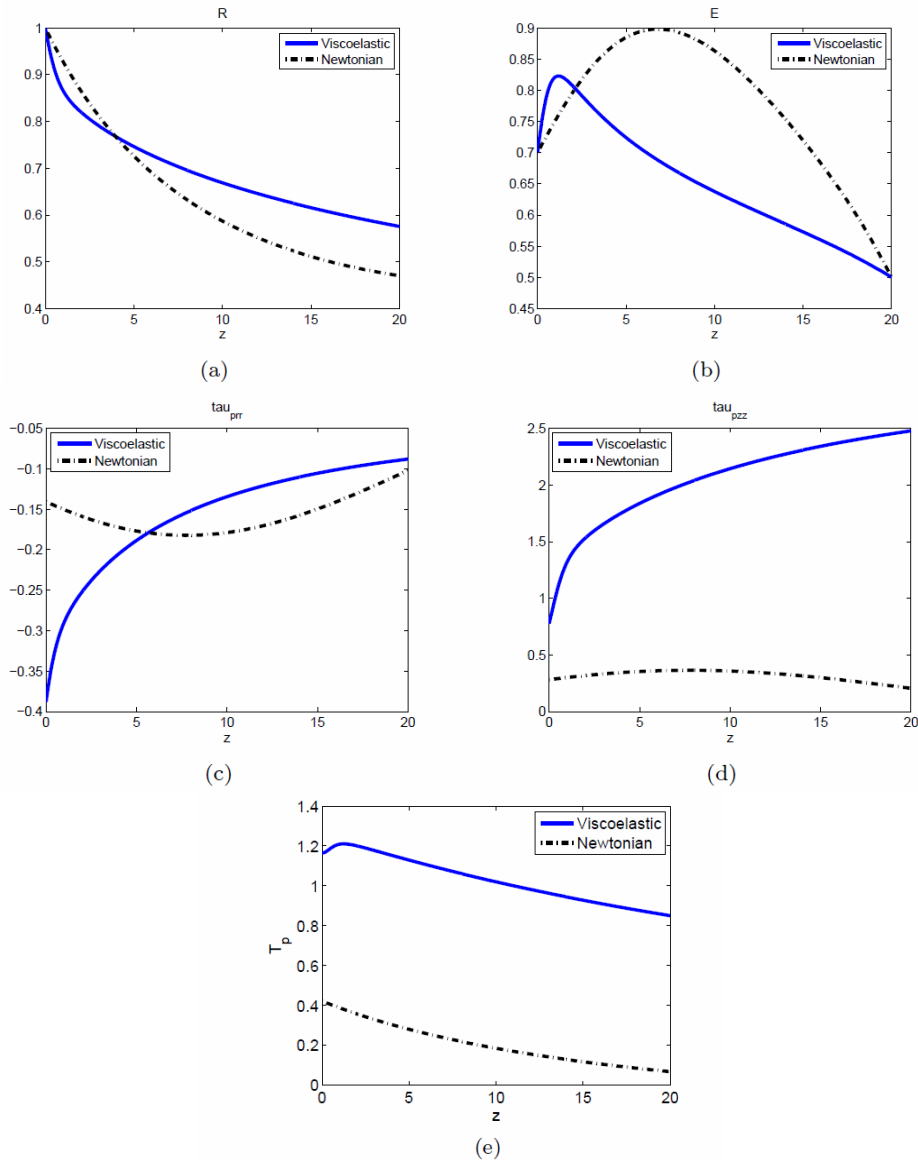


Figure 9: Solutions given by the viscoelastic model for Newtonian and viscoelastic cases (a) R; (b) E; (c) τ_{prr} ; (d) τ_{pzz} ; (e) T_p ³⁶

CONCLUDING REMARKS

Due to the rising interest in nanoscale materials and properties, research on the electrospinning process has intensified in recent years. Since the electrospinning process is dependent on a lot of different parameters, changing them will lead to significant variations in the process. In this paper, we have attempted to investigate some of the most important relationships from ongoing research into the fundamental physics that govern the electrospinning process. The idea has been to provide a few guiding principles to those who would use electrospinning to fabricate materials

with initial scrutiny. We have outlined the flow procedure involved in the electric field and those associated with the jetting process. The relevant processes are the steady thinning jet, whose behaviour can be understood quantitatively using continuum equations of electrohydrodynamics, and the ensuing fluid dynamical instabilities that give rise to whipping of the jet. The current carried by the jet is of critical importance to the process and some scaling aspects concerning the total measured current have been discussed. The basics of electrospinning modeling involve mass conservation, electric charge conservation, momentum balance, Coulomb’s law and

constitutive equations (Ostwald-de Waele power law, Giesekus equation and Maxwell equation), which are discussed in detail. These relations play an important role in setting the final features. The dominant balance of forces controlling the dynamics of the electrospinning process depends on the relative magnitudes of each underlying physical effect entering the set of governing equations. A model has been performed and simulated for a straight electrified fluid jet of

viscoelastic polymers by applying the relaxation method.

The model capability to predict the behavior of the process parameters was demonstrated using simulation in the last part. The plots obviously showed the changes of each parameter versus axial position. During the jet thinning, the electric field shoots up to a peak and then relaxes. The tensile force also has an initial rise and then reduces. All the plots show similar behaviour to those reported by other researchers.

SYMBOLS

| SI Units | Definition | Symbols |
|-------------------|--|--------------------------|
| M | Radius of jet | R |
| m/s | Jet velocity | v |
| m ³ /s | Flow rate | Q |
| A | Jet current | I |
| A/m ² | Current density | J |
| m ² | Cross-sectional area | $A(s), S$ |
| S/m | The conductivity of the liquid | K |
| V/m | Electric field | E |
| M | Spinning distance | L |
| C/m ² | Electric density | σ |
| kg m/s, (N.s) | Linear momentum | P |
| N | Force | F |
| S | Time | t |
| Kg | Mass | m |
| kg/m ³ | Density | ρ |
| m | Jet axial position | z |
| N/m ² | Pressure | p |
| N/m ² | Axial viscous normal stress | τ_{zz} |
| N/m | Surface tension | γ |
| - | Slope of the jet surface | R' |
| N/m ² | Tangential electric force | t_t^e |
| N/m ² | Normal electric force | t_n^e |
| - | Dielectric constant of the jet | ϵ |
| - | Dielectric constant of the ambient air | $\bar{\epsilon}$ |
| J | Electric work | W_e |
| m | Distance | l |
| J | Electric potential energy | U_e |
| N/m ² | Radial normal stress | τ_{rr} |
| C/m ² | Polarized charge density | ρ_p' |
| C/m ² | Polarization | P' |
| C | Charge | $q, q_0 \text{ \& } Q_b$ |
| m | Distance between two charges | r |
| kV | Electric potential | V |
| N/m ² | Shear stress | τ |
| - | Flow consistency index | K' |
| - | Flow behavior index | m |
| - | Constant | μ |
| s ⁻¹ | Rate of strain tensor | $\dot{\gamma}$ |
| N/m ² | Excess stress | S_k C_k |

| | | |
|-------------------|---------------------------------|----------------|
| N/m^2 | Configurational tensor | η |
| P | Viscosity | E_k |
| N/m^2 | Young's modulus | μ_k |
| N/m^2 | Shear modulus | β_k |
| $m^2/(V \cdot s)$ | Constitutive mobility | N |
| m^{-3} | Number of beads per unit volume | T |
| K | Temperature | G |
| N/m^2 | Elastic modulus | l |
| m | Filament | ε' |
| - | Lagrangian axial strain | b |
| - | Power exponent | |

REFERENCES

- ¹ D. H. Reneker and A. L. Yarin, *Polymer*, **49**, 2387 (2008).
- ² D. H. Reneker, A. L. Yarin, E. Zussman and H. Xu, *Adv. Appl. Mech.*, **41**, 343 (2007).
- ³ A. K. Haghi and G. Zaikov (Eds.), "Advances in Nanofibre Research", Smithers Rapra Technology, 2012, p. 194.
- ⁴ A. K. Haghi (Ed.), "Electrospinning of Nanofibers in Textiles", Apple Academic Press Inc., 2011, p. 132.
- ⁵ S. Maghsoodloo, S. Rafiei, S. Arbab, B. Noroozi and A. K. Haghi, *Polym. Res. J.*, **6**, 361 (2012).
- ⁶ A. Frenot and I. S. Chronakis, *Curr. Opin. Colloid. In.*, **8**, 64 (2003).
- ⁷ P. Fritzson (Ed.), "Principles of Object-Oriented Modeling and Simulation with Modelica 2.1", Wiley-IEEE Press, 2003, p. 944.
- ⁸ A. J. Collins, D. Meyr, S. Sherfey, A. Tolk and M. Petty, "The Value of Modeling and Simulation Standards", Virginia Modeling, Analysis and Simulation Center, Old Dominion University, 2011, pp. 1-8.
- ⁹ S. Robinson (Ed.), "Simulation: the Practice of Model Development and Use", Wiley, 2004, p. 722.
- ¹⁰ I. I. Carson and S. John, in *Procs. The 36th Winter Simulation Conference*, Washington, DC, December 8-11, 2004, pp. 9-16.
- ¹¹ J. Banks (Ed.), "Handbook of Simulation", Wiley Online Library, 1998, p. 342.
- ¹² A. B. Pritsker and B. Alan (Eds.), "Principles of Simulation Modeling", Wiley, 1998, p. 426.
- ¹³ C. P. Carroll (Ed.), "The Development of a Comprehensive Simulation Model for Electrospinning", 2009, p. 300.
- ¹⁴ A. Menon and K. Somasekharan, *Internet J. Bioengin.*, **4**, 10 (2009).
- ¹⁵ W. Gilbert (Ed.), "De Magnete", Dover Publications, Inc., 1958, p. 366.
- ¹⁶ N. Tucker, J. J. Stanger, M. P. Staiger, H. Razaq and K. Hofman, *J. Eng. Fiber. Fabr.*, **7**, 63 (2012).
- ¹⁷ J. Zeleny, *Phys. Rev.*, **3**, 69 (1914).
- ¹⁸ I. Hassounah (Ed.), "Melt Electrospinning of Thermoplastic Polymers", Aachen: Hochschulbibliothek Rheinisch-Westfälische Technischen Hochschule Aachen, 2012, p. 650.
- ¹⁹ G. I. Taylor (Ed.), "The Scientific Papers of Sir Geoffrey Ingram Taylor", Cambridge University Press, 1971, p. 590.
- ²⁰ L. Y. Yeo and J. R. Friend, *J. Exp. Nanosci.*, **1**, 177 (2006).
- ²¹ J. Miao, M. Miyauchi, T. J. Simmons, J. S. Dordick and R. J. Linhardt, *J. Nanosci. Nanotechnol.*, **10**, 5507 (2010).
- ²² W. E. Teo and S. Ramakrishna, *Nanotechnology*, **17**, 89 (2006).
- ²³ N. Bhardwaj and S. C. Kundu, *Biotechnol. Adv.*, **28**, 325 (2010).
- ²⁴ A. Greiner and J. H. Wendorff, *Angew. Chem. Int. Edit.*, **46**, 5670 (2007).
- ²⁵ N. M. Thoppey, R. E. Gorga, J. R. Bochinski and L. I. Clarke, *Macromolecules*, **45**, 6527 (2012).
- ²⁶ Y. Wan, J. Wei, J. Qiang, L. Yang, J. Fu *et al.*, *Adv. Sci. Lett.*, **10**, 590 (2012).
- ²⁷ L. Liu and Y. A. Dzenis, *Micro. Nano. Lett.*, **6**, 408 (2011).
- ²⁸ Z. M. Huang, Y. Z. Zhang, M. Kotaki and S. Ramakrishna, *Compos. Sci. Technol.*, **63**, 2223 (2003).
- ²⁹ S. Ramakrishna (Ed.), "An Introduction to Electrospinning and Nanofibers", World Scientific Publishing Company, 2005, p. 396.
- ³⁰ A. Arinsein, M. Burman, O. Gendelman and E. Zussman, *Nat. Nanotechnol.*, **2**, 59 (2007).
- ³¹ C. Lu, P. Chen, J. Li and Y. Zhang, *Polymer*, **47**, 915 (2006).
- ³² I. Greenfeld, A. Arinsein, K. Fezzaa, M. H. Rafailovich and E. Zussman, *Phys. Rev.*, **84**, 41806 (2011).
- ³³ R. H. M. Solberg, PhD Thesis, Department of Mechanical Engineering, Eindhoven University of Technology, 2007, p. 75.
- ³⁴ L. Gradoń, *Chem. Eng. Chem. Process. Technol.*, **1**, 1 (1914).

- ³⁵ R. B. Bird, W. E. Stewart and E. N. Lightfoot (Eds.), "Transport Phenomena", Wiley & Sons, Inc., 1960, p. 808.
- ³⁶ G. W. M. Peters, M. A. Hulsen and R. H. M. Solberg, "A Model for Electrospinning Viscoelastic Fluids", Department of Mechanical Engineering, Eindhoven University of Technology, 2007, p. 26.
- ³⁷ R. D. Whitaker, *J. Chem. Educ.*, **52**, 658 (1975).
- ³⁸ M. M. Hohman, M. Shin, G. C. Rutledge and M. P. Brenner, *Phys. Fluid.*, **13**, 2201 (2001).
- ³⁹ J. H. He, L. Xu, Y. Wu and Y. Liu, *Polym. Int.*, **56**, 1323 (2007).
- ⁴⁰ L. Xu, F. Liu and N. Faraz, *Comput. Math. Appl.*, **64**, 1017 (2012).
- ⁴¹ J. L. Heilbron (Ed.), "Electricity in the 17th and 18th Century: A Study of Early Modern Physics", University of California Press, 1979, p. 437.
- ⁴² S. Karra, Indian Institute of Technology. 2007, Texas A&M University. p.60.
- ⁴³ R. P. Feynman, R. B. Leighton, M. Sands and E. M. Hafner, *Am. J. Phys.*, **33**, 125 (1965).
- ⁴⁴ C. O. Bennett and J. E. Myers (Eds.), "Momentum, Heat, and Mass Transfer", McGraw-Hill, 1982, p. 848.
- ⁴⁵ R. P. Feynman, R. B. Leighton, M. Sands and E. M. Hafner, *Am. J. Phys.*, **33**, 750 (2005).
- ⁴⁶ J. J. Feng, *Phys. Fluid.*, **14**, 3912 (2002).
- ⁴⁷ S. H. Hou and C. K. Chan, *Appl. Math. Mech.*, **32**, 1515 (2011).
- ⁴⁸ J. C. Maxwell, Electrical Research of the Honorable Henry Cavendish, 426, Cambridge, 1878, UK.
- ⁴⁹ R. V. Vught, PhD Thesis, Department of Mechanical Engineering, Eindhoven University of Technology, 2010, p. 68.
- ⁵⁰ J. H. Jeans (Ed.), "The Mathematical Theory of Electricity and Magnetism", Cambridge University Press, 1927, p. 536.
- ⁵¹ D. H. Reneker, A. L. Yarin, H. Fong and S. Koombhongse, *J. Appl. Phys.*, **87**, 4531 (2000).
- ⁵² C. Truesdell and W. Noll (Eds.), "The Non-Linear Field Theories of Mechanics", Springer, 2004, p. 579.
- ⁵³ D. Roylance, Lecture Notes, Department of Materials Science and Engineering, Massachusetts Institute of Technology, 2000, p. 10.
- ⁵⁴ J. H. He, Y. Wu and N. Pang, *Int. J. Nonlin. Sci. Num.*, **6**, 243 (2005).
- ⁵⁵ R. W. Little (Ed.), "Elasticity", Courier Dover Publications, 1999, p. 431.
- ⁵⁶ P. Bhattacharjee, V. Clayton and A. G. Rutledge, in "Comprehensive Biomaterials", Elsevier, 2011, pp. 497-512.
- ⁵⁷ A. Clauset, C. R. Shalizi and M. E. J. Newman, *SIAM Rev.*, **51**, 661 (2009).
- ⁵⁸ K. Garg and G. L. Bowlin, *Biomicrofluidics*, **5**, 13403 (2011).
- ⁵⁹ A. F. Spivak and Y. A. Dzenis, *Appl. Phys. Lett.*, **73**, 3067 (1998).
- ⁶⁰ Y. Wan, Q. Guo and N. Pan, *Int. J. Nonlin. Sci. Num.*, **5**, 5 (2004).
- ⁶¹ H. Giesekus, *Rheol. Acta*, **5**, 29 (1966).
- ⁶² H. Giesekus, in "The Karl Weissenberg 80th Birthday Celebration Essays", edited by J. Harris and K. Weissenberg, East African Literature Bureau, 1973, pp. 103-112.
- ⁶³ J. M. Wiest, *Rheol. Acta*, **28**, 4 (1989).
- ⁶⁴ R. B. Bird and J. M. Wiest, *Annu. Rev. Fluid. Mech.*, **27**, 169 (1995).
- ⁶⁵ H. Giesekus, *J. Non-Newton. Fluid.*, **11**, 69 (1982).
- ⁶⁶ P. J. Oliveira, *Numer. Heat.Tr. B-Fund.*, **40**, 283 (2001).
- ⁶⁷ M. Simhambhatla and A. I. Leonov, *Rheol. Acta*, **34**, 259 (1995).
- ⁶⁸ H. Giesekus, *Rheol. Acta*, **21**, 366 (1982).
- ⁶⁹ J. J. Feng, *J. Non-Newton. Fluid.*, **116**, 55 (2003).
- ⁷⁰ A. C. Eringen and G. A. Maugin, in "Electrodynamics of Continua II", Springer, 1990, pp. 551-573.
- ⁷¹ K. Hutter, *SIAM Rev.*, **33**, 315 (1991).
- ⁷² G. Marrucci, *J. Rheol.*, **16**, 321 (1972).
- ⁷³ T. A. Kowalewski, S. Barral and T. Kowalczyk, *Procs. IUTAM Symposium on Modelling Nanomaterials and Nanosystems*, Aalborg, Denmark, May 19-22, 2009, pp. 279-292.
- ⁷⁴ B. Kuipers (Ed.), "Qualitative Reasoning: Modeling and Simulation with Incomplete Knowledge", MIT Press, 1994, p. 554.
- ⁷⁵ B. J. West, *Chaos. Soliton. Fract.*, **20**, 33 (2004).
- ⁷⁶ P. G. De Gennes and T. A. Witten (Eds.), "Scaling Concepts in Polymer Physics", 1980, p. 324.
- ⁷⁷ J. H. He, Y. Q. Wan and J. Y. Yu, *Int. J. Nonlin. Sci. Num.*, **5**, 243 (2004).
- ⁷⁸ J. H. He and H. M. Liu, *Nonlinear Anal.-Theor.*, **63**, 919 (2005).
- ⁷⁹ J. H. He, Y. Q. Wan and J. Y. Yuc, *Int. J. Nonlin. Sci. Num.*, **5**, 253 (2004).
- ⁸⁰ J. H. He and Y. Q. Wan, *Polymer*, **45**, 6731 (2004).
- ⁸¹ J. H. He, Y. Q. Wan and J. Y. Yu, *Polymer*, **46**, 2799 (2005).
- ⁸² R. Kessick, J. Fenn and G. Tepper, *Polymer*, **45**, 2981 (2004).
- ⁸³ D. F. Boucher and G. E. Alves (Eds.), "Dimensionless numbers", 1959, part 1 and 2.
- ⁸⁴ D. C. Ipsen (Ed.), "Units Dimensions and Dimensionless Numbers", McGraw Hill Book Company Inc., 1960, p. 466.
- ⁸⁵ H. L. Langhaar (Ed), "Dimensional Analysis and Theory of Models", Wiley, 1951, p. 166
- ⁸⁶ G. H. McKinley, *Bull. Soc. Rheol.*, **2005**, 6 (2005).
- ⁸⁷ C. P. Carroll, E. Zhmayev, V. Kalra and Y. L. Joo, *Korea-Aust. Rheol. J.*, **20**, 153 (2008).
- ⁸⁸ D. A. Saville, *Annu. Rev. Fluid. Mech.*, **29**, 27 (1997).

⁸⁹ J. I. Ramos, *Int. J. Numer. Meth. Fluids*, **23**, 221 (1996).

⁹⁰ J. W. Ha and S. M. Yang, *J. Fluid. Mech.*, **405**, 131 (2000).

⁹¹ T. Dasri, Walailak, *J. Sci. Technol.*, **9**, 287 (2012).

⁹² A. Holzmeister, A. L. Yarin and J. H. Wendorff, *Polymer*, **51**, 2769 (2010).

⁹³ C. J. Angamma and S. H. Jayaram, in *Procs. ESA Annual Meeting on Electrostatics*, Case Western Reserve University, Cleveland OH., June 14-16, 2011, pp. 1-9.

⁹⁴ C. J. Thompson, G. G. Chase, A. L. Yarin and D. H. Reneker, *Polymer*, **48**, 6913 (2007).

⁹⁵ L. Xu, Y. Wu and Y. Nawaz, *Comput. Math. Appl.*, **61**, 2116 (2011).